DOCKET FILE COPY ORIGINAL

UNITED STATES GOVERNMENT

M E M O R A N D U M

DATE: October 19, 1993

REPLY TO
ATTN OF: Robert Cleveland, SED, OET

SUBJECT: Items to be placed in Docket ET 93-62

TO: Secretary, FCC

The attached letter and two supporting documents from Professor Om P. Gandhi of the University of Utah, dated October 13, 1993, are relevant to the above-referenced docket that deals with new environmental guidelines for radiofrequency radiation. The Commission has proposed adopting new guidelines in our Notice of Proposed Rule Making in ET Docket 93-62 (FCC 93-142).

The originals plus four copies of this letter and the supporting documents are enclosed for incorporation into the docket record in this proceeding. If there are any questions please contact me at 653-8169.

ENCLOSURES

93-62

THE UNIVERSITY OF UTAH

October 13, 1993

EJ Doc-93-62

Dr. Robert F. Cleveland, Jr.
Federal Communications Commission
Office of Engineering & Technology
Mail Stop 1300 A2
1919 M Street, N.W.
Washington, D.C. 20554

Dear Bob:

I enclose herewith preprints of two recent papers that have been submitted for publication to *IEEE Transactions on Electromagnetic Compatibility.*

You may find these papers of interest in connection with the FCC Notice of Proposed Rule Making.

Sincerely,

OM P. GANDHI
Professor and Chairman

OPG:jk

Enclosures

Department of Electrical Engineering
3280 Merrill Engineering Building
Salt Lake City, Utah 84112
(801) 581-6941

INDUCED FOOT-CURRENTS IN HUMANS EXPOSED TO RADIO-FREQUENCY EM FIELDS

S. Tofani[1], G. D'Amore[1], G. Fiandino[1], A. Benedetto[1],
O. P. Gandhi[2], and J. Y. Chen[2]
(1) Laboratorio di Sanità Pubblica - Sezione Fisica, 10015 Ivrea, Italy
(2) Department of Electrical Engineering
University of Utah
Salt Lake City, Utah 84112, U.S.A.

ABSTRACT

Because of the strong relationship of the foot currents to the highest SARs in the human body, limits on these currents have been prescribed in the ANSI/IEEE Safety Standard for frequencies up to 100 MHz. We have measured the induced currents passing through the human feet for nine subjects exposed to vertically polarized electric fields close to transmitting antennas in the FM band 90-104 MHz. The experimental results are in excellent agreement with the numerical values obtained using an anatomically based model and the FDTD method both for the average male height of 1.75 m and the tallest experimental subject of height 1.91 m. Currents in excess of the RF safety guidelines would result both for controlled and uncontrolled environments if the incident electric fields were purely vertical and of maximum values given in the safety guidelines. It is important therefore to measure not only the E- and H-fields, but also the induced currents up to the recommended maximum frequency of 100 MHz and perhaps for the entire FM/TV based up to 110 MHz.

EVALUATION OF INDUCED FOOT-CURRENTS IN HUMANS EXPOSED TO RADIO-FREQUENCY EM FIELDS

INTRODUCTION

Because of its relationship to electromagnetic power deposition (specific absorption rates or SARs) in the human body, determination of the currents passing through the feet has become an important parameter for assessment of radiofrequency (RF) hazards. Limits of the foot currents have therefore been recommended in the recently approved ANSI-IEEE Safety Standard [1] in addition to the maximum values of electric and magnetic fields. The maximum total current for both feet suggested in the safety guidelines is 200 mA and 90 mA for controlled and uncontrolled environments, respectively.

Several papers have previously reported on the theoretical and experimental evaluation of the currents induced in the human body for exposure to plane-waves and for leakage electromagnetic (EM) fields of RF dielectric heaters [2-7]. However, there is lack of experimental data on foot currents induced by RF EM fields for frequencies in excess of 50 MHz [2]. Since the induced currents for male adults have been found to diminish for frequencies in excess of the grounded resonance frequency of 40 MHz, the lack of experimental data has led some to question the need for foot current measurements up to 100 MHz recommended in the ANSI-IEEE Safety Standard [1]. The focus of this paper is to give the experimental data on the measured foot currents for exposure to EM fields in the important FM broadcast band 90-104 MHz and to compare this data with the induced current distributions using the existing numerical methods. The data show that substantial currents would indeed be induced in the human body for the electric fields suggested in the safety guidelines. Since these currents would be in excess of the induced current limits recommended in the safety guidelines if the incident electric fields were to be vertical, measurement of foot currents is indeed necessary for frequencies up to 104 and perhaps to 110 MHz to ensure that the current limits in the safety standard are not exceeded.

EXPERIMENTAL MATERIALS AND METHODS

Foot currents were measured in outdoor electromagnetic environments characterized by the presence of multiple-source, multiple-frequency EM fields produced by antennas transmitting radio programs in the FM broadcast band (90-104 MHz). The antennas were made of vertical dipoles.

For measurements we have used a stand-on current dosimeter developed at the University of Utah[2], which consists of a polyethylene sheet of thickness 6 mm that was sandwiched between the copper plates of size 30 x 30 cm, placed in series with an RF milliammeter. The human body induced current through both feet to ground was determined by having a person stand on the top copper plate, the bottom plate being placed on the ground over an additional copper sheet of 50 x 50 cm to improve the grounding effect.

To evaluate the foot current induced in a human body exposed to multiple-source multiple-frequency EM field, we have made a spectral analysis of foot current connecting a spectrum analyzer (model HP 8562A) directly to the two copper plates of the dosimeter, whose impedance is 6 Ω at the considered frequencies.

The foot-current dosimeter was calibrated in the laboratory to evaluate its response versus amplitude and frequency of the current. The calibration has been made injecting in the dosimeter a known current produced by signal generator HP 8656B. The experimental set up for this calibration is shown in Fig. 1.

In the calibration curve shown in Fig. 2 the dosimeter reading as a function of the frequency, for different amplitudes of the injected current, are given. From this figure we can see that the dosimeter response is almost independent (within 5 percent) of the frequency in the considered frequency range. It can be observed also that the meter reading is accurate (within 5 percent) at 30 and 50 mA, while the current is increasingly overestimated by the meter above 50 mA reaching an overestimation of 11 percent at a current amplitude equal to 90 mA.

The total current evaluated from data obtained using the spectrum analyzer was compared with the total current measured by the dosimeter. To increase the accuracy we accepted only data in agreement between the two measurement systems.

Foot current was measured for nine subjects having different heights and areas A of the ankle sections. For each measurement point and frequency we evaluated the parameter $F_\nu = I_\nu/E_z$ where I_ν is the foot current at a fixed frequency ν, and E_z is the vertical component of the electric field.

The vertical component of the electric field was measured following the procedures reported in [8].

NUMERICAL COMPUTATIONS

The procedure used for numerical computations has been described in detail in several of our earlier publications [3-6] and would therefore not be given here. For the present computations we have used an anatomically based model of the human body where the tissue compositions have been prescribed for each of the subvolumes of the body or cells of dimension 1.31 x 1.31 x 1.31 cm. As previously described [6], the tissue compositions were obtained from the anatomical cross sectional diagrams of the human body [9]. This model consisting of 134 layers has a height of 175.5 cm and weight 69.6 kg. Without changes in the human anatomy this model can be used to obtain scaled models with slightly different heights and cross sectional dimensions, respectively. By changing the cell size δ_z in the vertical (z-) direction from 1.31 cm to 1.425 cm, the height of the 134 layer model can for example, be increased to 191 cm to correspond to the height for the tallest of the experimental subjects. Similarly we can increase the cell size for the cross sectional planes $\delta_x = \delta_y$ from 1.31 cm to 1.546 cm to obtain the single-ankle cross sectional area A represented by 28 cells to be 66.9 cm^2 which once again, corresponds to the ankle cross sectional area for this 1.91-m tall individual who participated in the experiments.

For calculation of the induced electric field components we have used the well-established finite-difference time-domain (FDTD) method which has also been described in our earlier papers [3-6] and many other publications in the literature. As described previously [6] we have used the internal E-fields to calculate the local vertical (z-directed) current densities J_z which were then used to obtain the vertical currents induced for the various layers. Consistent with the experimental conditions, we have considered the grounded models for the numerical computations. This was done to assess the worst case exposure of the individuals and also in recognition of the fact that shoe-wearing conditions do not result in substantial reductions (less than 15-20 percent) of the foot currents for frequencies in excess of 30 - 40 MHz [2].

RESULTS AND DISCUSSION

In Fig. 3 we give the measured data as a function of frequency. Curve A gives the mean data for all nine subjects which had an average height of 1.75 m while curve B gives the data for the tallest of the subjects who had a height of 1.91 m. In Figs. 4 and 5 we give the calculated induced current variations for models of height 1.75 m and 1.91 m, respectively, for a vertically polarized incident field E_z = 1 V/m (rms) at frequencies varying from 90 to 110 MHz. In Table 1 we compare the experimentally and numerically determined values of F_v at various frequencies. The agreement between the experimental and numerical values of F_v is excellent.

We can see that the mean values of F_v for the various subjects decreases with frequency, ranging from 4.46 to 3.45 in the frequency range 90 to 104 MHz. For a maximum permissible electric field value of 61.4 V/m given in the ANSI/IEEE safety guidelines [1] for the controlled environments, this will imply an induced current of 212-274 mA which is in excess of the 200 mA limiting value that has been recommended in the safety guidelines for these environments. Similarly for the maximum permissible exposure of 27.5 V/m in uncontrolled environments, the induced currents of 95-123 mA will also exceed the limiting value of 90 mA for these exposure conditions. For the tallest individual

of height 1.91 m the currents will be even larger and on the order of 134 -149 mA in the frequency band 90-100 MHz for the uncontrolled environments. Both of these values are in excess of 90 mA suggested as the current limit in the ANSI/IEEE safety guidelines.

CONCLUSIONS

Both the experimental data and the numerical calculations point to the need for induced foot current measurements for frequencies up to 100 MHz or perhaps through the entire FM/TV band up to 108-110 MHz. From the results presented in this paper it is obvious that substantial currents may indeed be induced in the human and that these currents will be in excess of the ANSI/IEEE limits of the foot currents if the incident fields were vertical and relatively uniform over the extent of the human body.

ACKNOWLEDGEMENT

Gandhi and Chen's work on this project was supported by National Institute of Environmental Health Sciences, Research Triangle Park, North Carolina (USA) under Grant ES -03329.

REFERENCES

[1] ANSI (1991): "American National Standard Safety Levels with Respect to Human Exposure to Radio Frequency Electromagnetic Fields (3 kHz - 300 GHz). ANSI C95.1.

[2] Gandhi, O. P., Chen, J. Y., and Riazi, A. (1986): "Currents Induced in a Human Being for Plane-Wave Exposure Conditions 0-50 MHz and for RF Sealers. *IEEE Transactions on Biomedical Engineering,* Vol. 33, pp. 757-767.

[3] Chen, J. Y., and Gandhi, O. P., (1989): "Electromagnetic Deposition in an Anatomically Based Model of Man for Leakage Fields of a Parallel-Plate Dielectric Heater." *IEEE Transactions on Microwave Theory and Techniques,* Vol. 37, pp. 174-180.

[4] Chen, J. Y., and Gandhi, O. P. (1989): "RF Currents Induced in an Anatomically Based Model of a Human for Plane-Wave Exposures (20-100 MHz). *Health Physics*, Vol. 57, pp. 89-98.

[5] Chen, J. Y., Gandhi, O. P., and Conover, D. L., (1991): "SAR and Induced Current Distributions for Operator Exposure to RF Dielectric Sealers." *IEEE Transactions on Electromagnetic Compatibility*, Vol. 33, pp. 252-261.

[6] Gandhi, O. P., Gu, Y. G., Chen, J. Y., and Bassen, H. I. (1992): "Specific Absorption Rates and Induced Current Distributions in an Anatomically Based Human Model for Plane-Wave Exposures." *Health Physics*, Vol. 63, pp. 281-290.

[7] Conover, D. L., Moss, C. E., Murray, W. E., Edwards, R. M., Cox, C., Grajawski, B., Warren, D. M., and Smith, J. M., (1992): "Foot Currents and Ankle SARs Induced by Dielectric Heaters," *Bioelectromagnetics,* Vol. 13, pp. 103-110.

[8] Tofani, S., and Ossola, P., (1992): "Accuracy in Outdoor Isotropic Measurements of Multiple-Source, Multiple-Frequency EM Fields," *IEEE Transactions on Electromagnetic Compatibility,* Vol. 34, pp. 299-303.

[9] Eycleshymer, A., and Schoemaker, D. M., (1970): "A Cross-Section Anatomy, New York: D. Appleton.

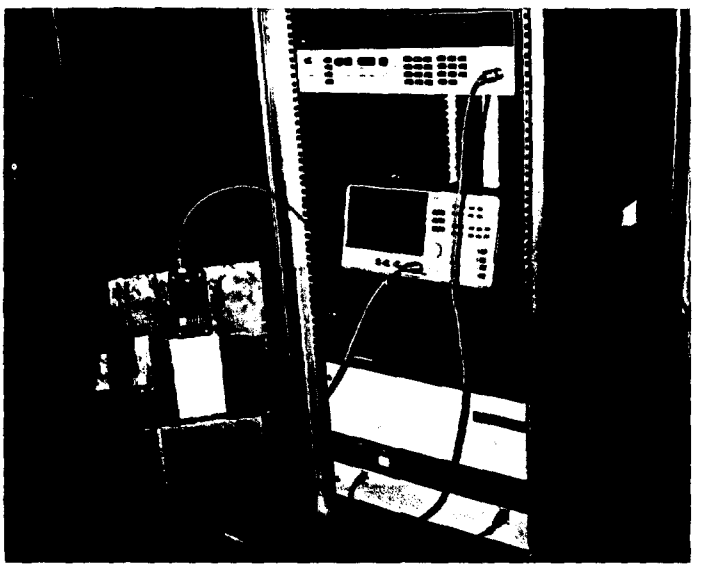

Fig. 1. The experimental set up for calibration of the dosimeter. The current is injected in the dosimeter by the two copper plates shown at the left of the dosimeter itself, which is connected via coaxial cable to the spectrum analyzer.

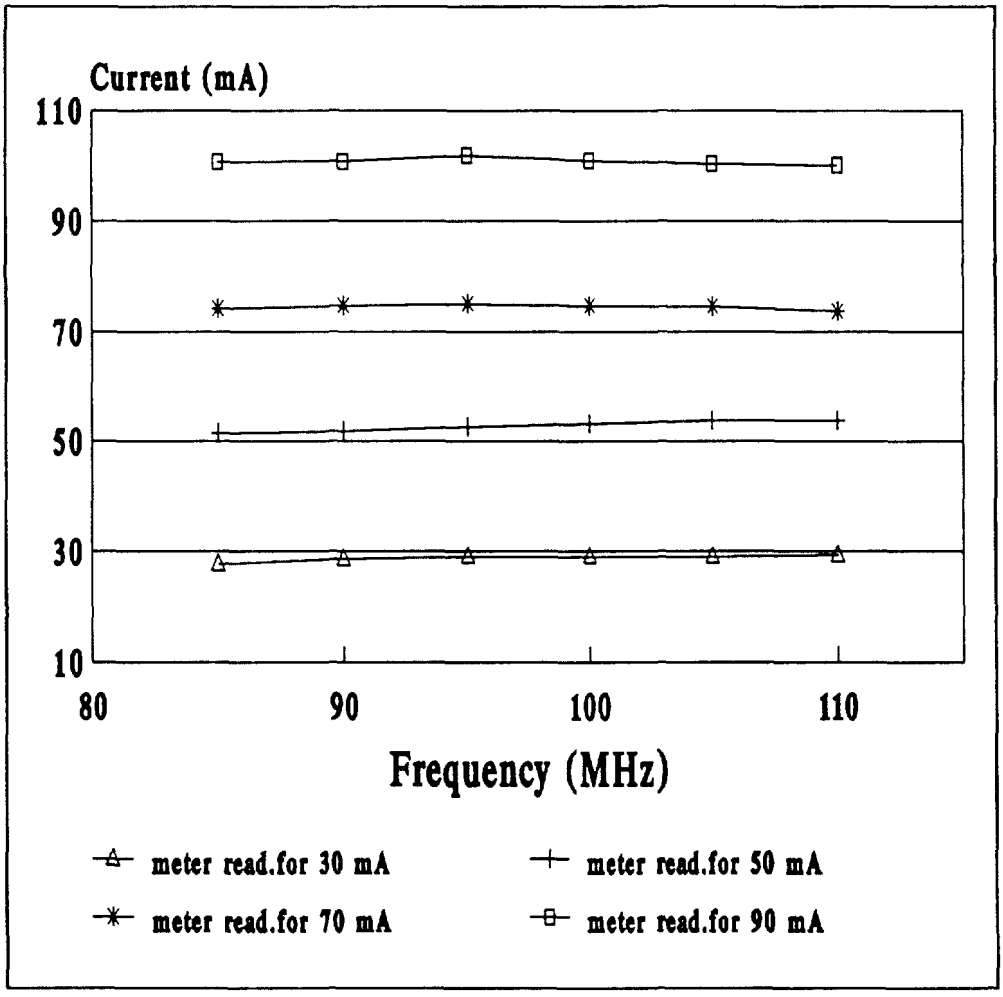

Fig. 2. Dosimeter reading as a function of frequency for four different amplitudes of the injected current.

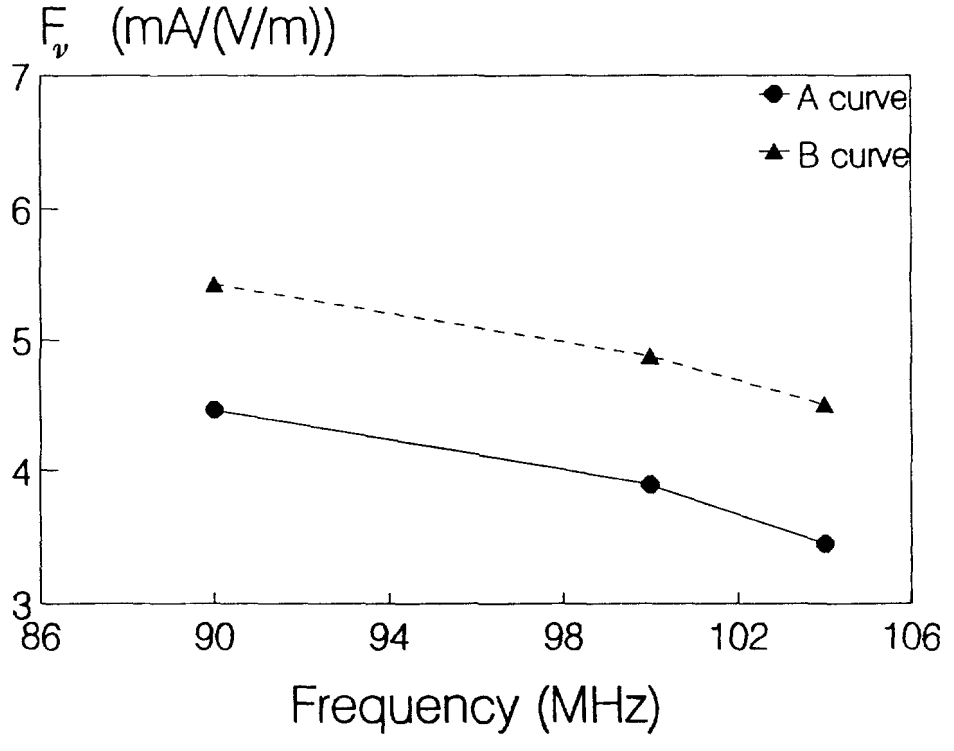

Fig. 3. Experimental foot currents for grounded subjects as a function of frequency; A curve shows the mean data for all nine subjects with an average height of 1.75 m; B curve shows the data for the tallest subject who had a height of 1.91 cm.

Table 1. Comparison of the experimental and numerical values of F_v at various frequencies for human subjects of height h.

Frequency MHz	Experimental F_v, mA/(V/m)		Numerical F_v, mA/(V/m)	
	h = 1.75 m	1.91 m	1.75 m	1.91 m
90	4.46	5.42	4.38	5.11
95	-	-	4.10	4.90
100	3.90	4.87	3.97	4.64
104	3.45	4.45	3.85	4.35
105	-	-	3.84	4.28
110	-	-	3.78	3.88

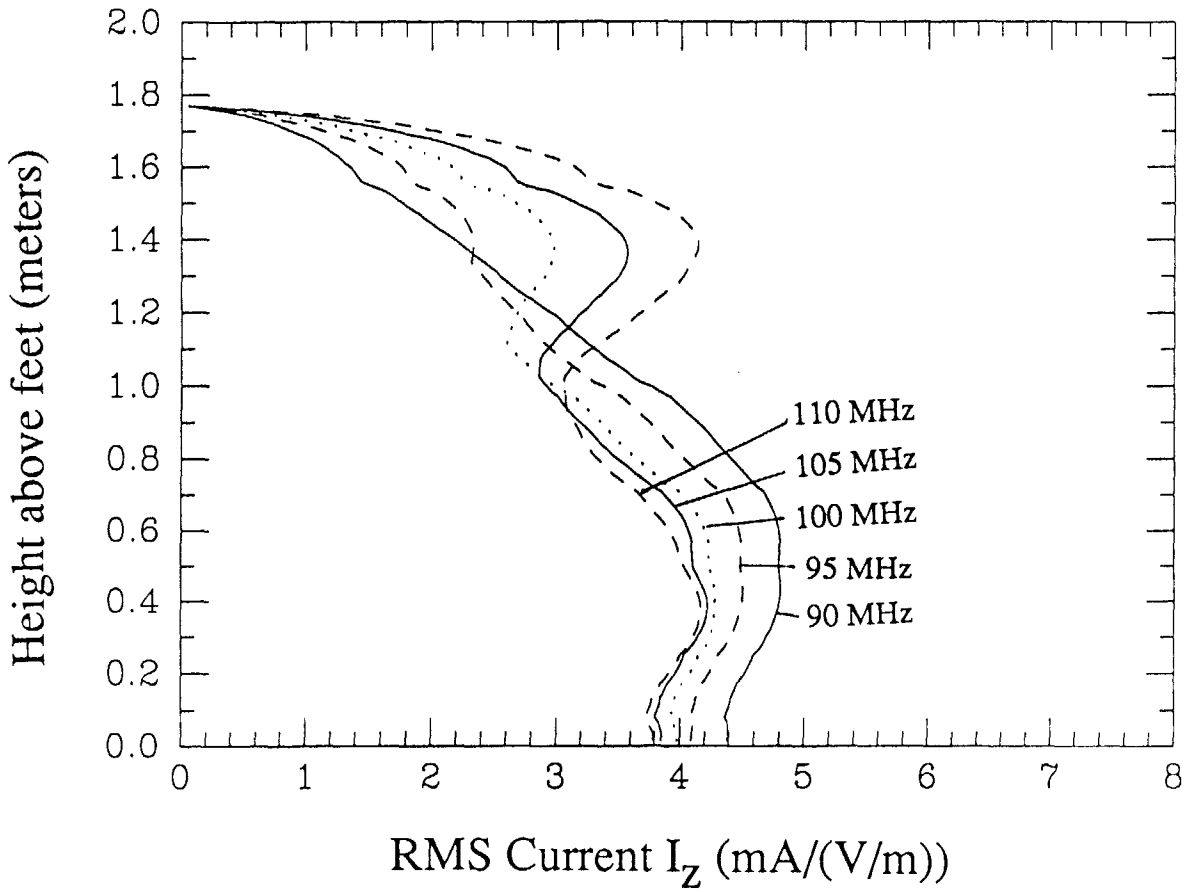

Fig. 4. Induced RF current variations for a grounded 1.75 m-tall anatomically based model of the human body for the frequency band 90-110 MHz.

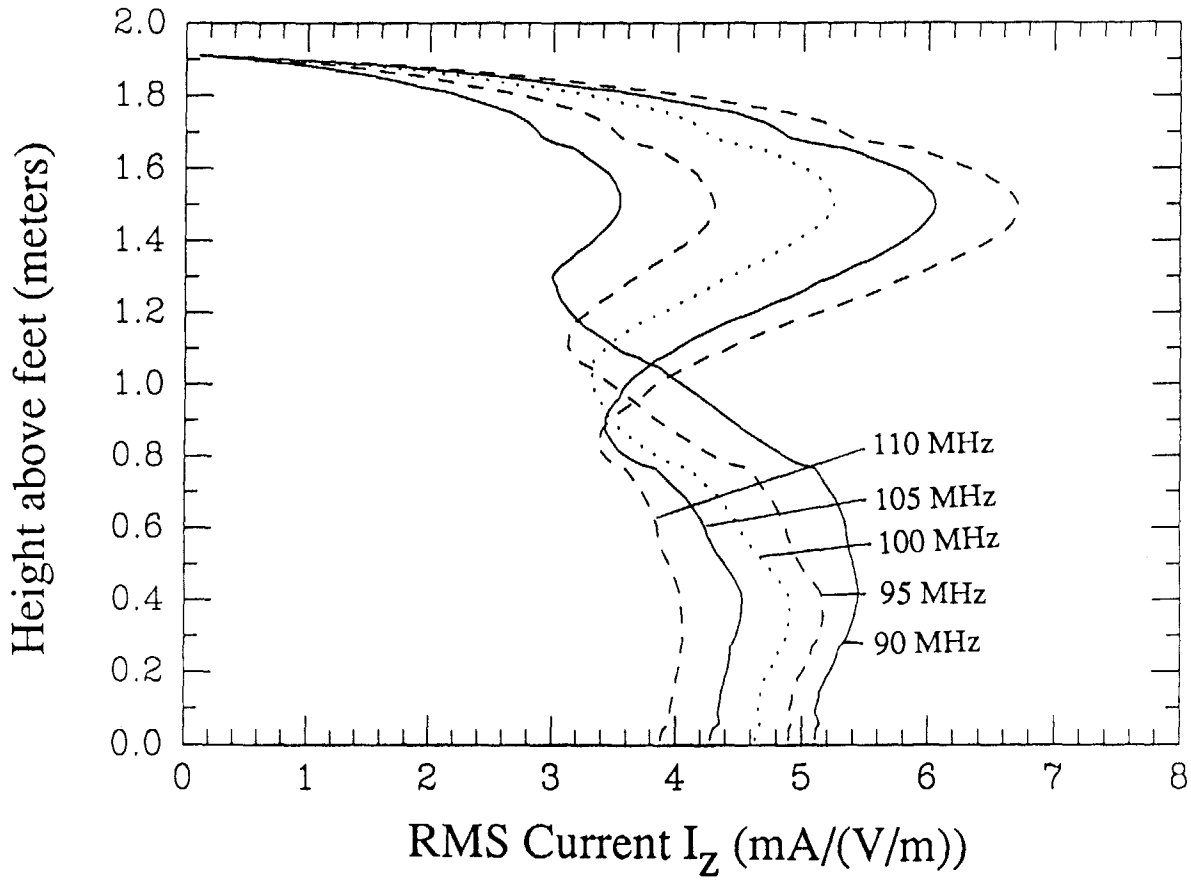

Fig. 5. Induced RF current variations for a grounded 1.91 m-tall anatomically based model of the human body for the frequency band 90-110 MHz.

ELECTROMAGNETIC ABSORPTION IN THE HUMAN HEAD FOR A PROPOSED 6 GHz HANDSET

Om P. Gandhi and Jin-Yuan Chen
Department of Electrical Engineering
University of Utah
Salt Lake City, Utah 84112

93-62

Abstract

We have used a new millimeter-resolution MRI-based model of the human body to calculate electromagnetic absorption in the head and neck for three 2-element Yagi antennas proposed for the handsets of a 6 GHz PCN trial system. The SAR distributions are obtained with a resolution of $1.974 \times 1.974 \times 1.5$ mm for the handsets that are held against the ears and tilted forward by 33°. The finite-difference time-domain technique is used to calculate the EM fields and SARs for the handset, antenna, and head and neck coupled region that is divided into $158 \times 84 \times 188$ or nearly 2.5 million cells. The highlights of the numerical calculations are verified by means of a head-shaped experimental model made of tissue-equivalent materials simulating the electrical properties (ε_r, σ) of skull, brain, muscle, eyes, and ears developed for use at 6 GHz. Because of the proximity to the antenna, the highest SARs are obtained for the upper ear. For a planned radiated power of 0.6 W, the peak SAR averaged over any 1 g of tissue defined as a tissue volume in the shape of a cube is less than the ANSI/IEEE C95.1-1992 safety guideline of 1.6 W/kg. Also, the whole-body-average SAR is at least two orders of magnitude less than 0.08 W/kg prescribed in the safety guideline.

I. Introduction

Higher microwave frequency personal communication networks (PCN) are being investigated for portable wireless communications of the future. To establish the feasibility of such a system, an experimental PCN system is being evaluated by AT&T Bell Laboratories. We have evaluated the electromagnetic absorption in the human head and the body vis à vis the ANSI/IEEE C95.1-1992 RF safety guidelines [1]. These safety

guidelines are given in terms of maximum permissible exposures (MPE) of electric field (E), magnetic field (H), or of power density (S) for controlled and uncontrolled environments. Though simple to use for far-field, relatively uniform exposures, the MPE limits are not easy to use for highly nonuniform fields such as in the near-field region of a proposed PCN handset. An alternative procedure given in the following [1] has, therefore, been suggested to satisfy the safety guidelines for uncontrolled environments which are defined as locations or situations where there is the exposure of individuals who have no knowledge or control of their exposure.

> An exposure condition can be considered to be acceptable if it can be shown that it produces mass-normalized rates of energy absorption (specific absorption rates or SARs) "below 0.08 W/kg, as averaged over the whole body, and spatial peak SAR values not exceeding 1.6 W/kg, as averaged over any 1 g of tissue (defined as a tissue volume in the shape of a cube), except for the hands, wrists, feet, and ankles, where the spatial peak SAR shall not exceed 4 W/kg, as averaged over any 10 g of tissue (defined as a tissue volume in the shape of a cube)."

For frequencies between 3,000-15,000 MHz, the averaging time for SARs is 90,000/f minutes where the frequency f is in MHz. For a proposed handset operating at 6 GHz, the averaging time, therefore, is 15 minutes.

Great strides have been made in the development of numerical methods that allow us to obtain quantitative information on SARs in anatomically based models of the human body or parts thereof for far-field or near-field exposure conditions [2]. Experimental techniques have also been developed to determine the SAR distributions using homogeneously or heterogeneously filled models [3-6]. In the most sensitive technique, the SARs are obtained from the internal electric fields (E) that can be measured by high-sensitivity implantable E-field probes, such as model BRH-15 [7], and using the relationship $SAR = \sigma E^2/\rho$ where σ is the conductivity of the tissue-simulant material and ρ is its mass density.

We have used the previously tested finite-difference time-domain (FDTD) numerical technique together with a newly developed millimeter-resolution model of the human body to obtain SAR distributions for three alternative antenna configurations that are being considered for the PCN handset. Since compositions were not available to simulate the various tissues at 6 GHz, new tissue-simulant materials were developed to simulate complex permittivities of brain, muscle, eyes, ears, and skull. Experimentally determined SARs for a head-shaped heterogeneous model were found to be in reasonable agreement with numerically calculated values. For a planned maximum radiated power of 0.6 W, whole-body-average SAR is not the issue since it is orders of magnitude smaller than 0.08 W/kg suggested in the ANSI safety guidelines. The more crucial quantity is the spatial-peak SAR as averaged over any 1 g of tissue taken in the shape of a cube. For all of the antenna and handset configurations, the spatial-peak SARs were found to be less than the 1.6 W/kg limit given in the ANSI safety guidelines.

II. The Finite-Difference Time-Domain Method

One of the most successful and versatile methods for SAR calculations is the finite-difference time-domain (FDTD) method [2, 8, 9]. This method was first proposed by Yee [10] and later developed by Taflove and colleagues [11-14], Holland [15], and Kunz and Lee [16]. We have extended the method for calculations of the distributions of electromagnetic (EM) fields and SARs in anatomically based models of the human body for whole-body or partial-body exposures due to far-field or near-field irradiation conditions [8, 9, 17, 18]. In this method, the time-dependent Maxwell's curl equations

$$\nabla \times \mathbf{E} = -\mu \frac{\partial \mathbf{H}}{\partial t} \quad , \quad \nabla \times \mathbf{H} = \sigma \mathbf{E} + \varepsilon \frac{\partial \mathbf{E}}{\partial t} \tag{1}$$

are implemented for a lattice of subvolumes or "cells" that may be cubical or parallelepiped with different dimensions δ_x, δ_y, and δ_z in x-, y-, or z-directions, respectively. The details

of the method are given in several of the above referenced publications and will, therefore, not be repeated here.

In the FDTD method it is necessary to represent not only the scatterer/absorber such as the human body or a part thereof, but also any near-field source/s such as a monopole antenna with or without a reflector and the supporting structure by means of the volume-averaged electrical properties (ε_r, σ). The source–body interaction volume is subdivided into the Yee cells. The interaction space consisting of several hundred thousand to a few million cells is truncated by means of absorbing boundaries. Initial fields often assumed to be sinusoidally varying are tracked in time for all cells of the interaction space. The problem is considered completed when a sinusoidal steady-state behavior for **E** and **H** is observed for the interaction space.

III. A New High-Resolution Model of the Human Body

In collaboration with Dr. James Lee of the Medical Imaging Laboratory, School of Medicine, and Professor Mark Nielson of the Department of Biology, University of Utah, we have developed a new millimeter-resolution model of the human body from the magnetic resonance imaging (MRI) scans of a male volunteer of height 176.4 cm and weight 64 kg. The MRI scans were taken with a resolution of 3 mm along the height of the body and 1.875 mm for the orthogonal axes in the cross-sectional planes. Even though the height of the volunteer was quite appropriate for an average adult male, the weight was somewhat lower than an average of 71 Kg, which is generally assumed for an average male. This problem can, to some extent, be ameliorated by assuming that the cell dimensions for the cross sections are larger than 1.875 mm by the ratio of $(71/64)^{1/2} = 1.053$. By taking the larger cell dimensions of $1.053 \times 1.875 = 1.974$ mm for the cross-sectional axes, the volume of the model can be increased by $(1.053)^2 = 1.109$, i.e., by about 10.9 percent which results in an increase of its weight by approximately the same percentage, i.e., to a new weight of approximately 71 Kg. The MRI sections were

converted into images involving 29 tissue types whose electrical properties can then be prescribed at the irradiation frequency. The tissue types are fat, muscle, bone, cartilage, skin, brain, nerve, cerebral spinal fluid (CSF), intestine, spleen, pancreas, heart, blood, eye, eye humor, eye sclera, eye lens, ear, liver, kidney, lung, bladder, stomach, ligament, compact bone, testicle, spermatic cord, prostate gland, and erectile tissue. For the present calculations we have used parts of the new model corresponding to the head and neck. A typical cross section of the new model of the body is shown in Fig. 1. This corresponds to a section through the eyes. Shown in Fig. 1 are the contours for the various features of this cross section such as the eyes, ear, nasal cavity, brain, etc. The various tissue types used for the different cross-sectional scans of the head and neck are given in Table 1. Also given there are the electrical properties that have been assumed for the various tissues at the handset frequency of 6 GHz [19, 20, 21]. Since the vertical resolution of 3 mm is not sufficient to model the driven element of the two-element Yagi antennas (about 12 mm in height) accurately, we have subdivided the thickness between each of the sections into two halves each of thickness 1.5 mm. The new dimensions for each of the cells, therefore, are $1.974 \times 1.974 \times 1.5$ mm along x, y, and z directions, respectively. The entire volume for the model of the head and neck is represented by $112 \times 98 \times 176 = 1{,}931{,}776$ cells. Because of the highly superficial nature of electromagnetic deposition at the high frequencies on the order of six gigahertz, it is sufficient to use half of the volume of the head for the side that is closest to the handset. For example, see the SAR distributions calculated for one of the antennas in Fig. 9 for three representative cross sections of the head -- layer nos. 60, 69, and 75, respectively. Layer no. 69 is in the xy plane containing the driving point of the antenna, while layers 60 and 75 are 1.35 cm above and 0.9 cm below this plane, respectively. It is interesting to note that the SARs exist for the layer of the skin and the surface of the brain with very little energy deposited both for the internal tissues and for the lower-conductivity skull.

IV. Test Runs

To verify the accuracy of the FDTD method, we have made several test runs to compare the results with known analytical solutions for these relatively simple geometries. Some of these test runs are described in the following:

1. We have calculated the current distribution for a quarter-wave monopole antenna above ground at 6 GHz. For these calculations, the linear 12.5-mm-tall antenna, assumed oriented along the z-axis, was represented by 13 cubical cells, each of dimension 0.9615 mm. The bottommost cell (numbered 0) close to the ground plane was air filled, while for the upper 12 cells, the tangential fields E_x and E_y were equated to zero in recognition of the fact that these cells are made of highly conducting metal. A sinusoidal driving voltage was assumed across the gap for cell number 0. Starting with this prescribed uniform z-directed E-field for cell number 0, the various components of **E** and **H** were calculated in the surrounding space. From the calculated tangential magnetic fields, we obtained the z-directed current flowing through each of the antenna cells from the expression

$$I = -\int \mathbf{H} \bullet d\ell \tag{2}$$

The normalized currents for various cells are plotted in Fig. 2 and compared against the expected quarter-wave cosine distribution of current plotted as a solid curve. The agreement is good. From these calculations, we can also calculate the complex feed-point impedance by dividing the driving-point voltage by the current through cell number 0. For this square cross-section quarter-wave monopole, we calculate a driving-point impedance of 30.3 + j37.9

ohms, which compares favorably with a theoretical impedance of 36.5 + j21 ohms for a thin-wire antenna of the same length.

2. We have run a second test case to calculate the depth of penetration in a lossy material. It was argued that by using the model of a slab with dielectric properties corresponding to two-thirds muscle at 6.0 GHz (ε_r = 29.0 and σ = 3.15 S/m [19]), we can compare the 1/e depth of penetration obtained by the FDTD method with that given analytically for plane waves. From electromagnetic theory, for a plane wave propagating in the y direction (see the insert of Fig. 3), the propagation constant in the slab is given by

$$K = \left[-j\,\omega\,\mu_0\,(\sigma + j\,\omega\,\varepsilon_0\,\varepsilon_r)\right]^{1/2} = K' - j\,K'' \tag{3}$$

For the slab parameters ε_r = 29.0 and σ = 3.15 S/m at 6.0 GHz, the wave amplitude in the material will diminish as $e^{-K''y}$ or $e^{-108.8y}$ where y is in meters. In Fig. 3, we plot the FDTD-calculated values shown by dots and compare the same with the analytical variation given by $e^{-108.8y}$ at 6 GHz. The agreement can be seen to be very good.

After validating the accuracy of the FDTD method, we next calculated the coupling of the electromagnetic fields generated by a typical two-element Yagi antenna to this slab model. The height of the driven element was taken to be 12 mm and that for the reflector was 24 mm with the antenna-to-reflector spacing of 12 mm (~ λ/4). Spacing of the reflector antenna to the front surface of the slab was taken to be 16 mm (8 cells). The antenna was based on a metallic box of prescribed dimensions 5.59 × 4.83 × 16.38 cm which was represented by a high conductivity volume of 24 × 28 × 82 cubical cells (cell size = 2 mm). The total modeled volume along x, y, and z directions, respectively, was divided into 108 × 82 × 128 = 1,133,568 cells, with the slab model occupying

dimensions of 100 × 25 × 119 cells along the three axes, respectively. The calculated results are plotted also in Fig. 3. As seen in Fig. 3, attenuation of the fields in the slab due to the Yagi antenna is somewhat faster than that for plane waves. Whereas the 1/e depth of penetration due to plane waves is 9.2 mm, that for the fields due to this Yagi antenna is considerably shallower and is only on the order of 4.9 mm. This result of a reduced depth of penetration as compared to that for plane waves has previously been reported for electromagnetic fields of transverse dimensions less than a free space wavelength [22].

3. Yet another test case was that for a muscle-equivalent sphere where the three-dimensional distribution of fields can be compared with those obtained from the analytical Mie series solution [23]. Shown in Figs. 4a and 4b are the calculated variations of the magnitude of E_z along y and E_y along z for the central axes of the sphere, respectively. The properties taken for the sphere are: diameter = 0.1 m, ε_r = 29.0, and σ = 3.15 S/m. The electrical properties ε_r and σ correspond to those for 2/3 muscle at 6.0 GHz. Assumed for the calculations is a z-directed incident E-field of 1 V/m. Since the rest of the components are relatively small along the two central axes, these components are not shown.

   From Figs. 4a and 4b, one can see that a cell size δ = 2 mm, which is only as large as $\lambda_\varepsilon/4.5$ gives variations of the internal fields that are in reasonable agreement with those obtained analytically. Here, λ_ε is the wavelength within the tissue-simulant material that has been assumed for the model. A very similar result has also been previously observed [18] where we found that cell sizes on the order of $\lambda_\varepsilon/4$ give SAR distributions that were reasonably accurate and in good agreement with those given for smaller cell sizes.

V. Calculations of SAR Distributions

We have used three different antenna arrangements for calculations of SAR distributions in the MRI-based model of the human head where the tissue properties are prescribed for cells of dimensions $1.974 \times 1.974 \times 3$ mm. To simulate a handset that is typically tilted forward by about 33° for a vertically erect head, we have modified the MRI-based model so that it is tilted forward by 33°. With this forward tilt of the model, the handset may then be held in the vertical position for SAR calculations. This 33° forward tilt in the model of the head was accomplished by displacing each successive layer of the MRI scans separated by 3 mm back by 1 cell, i.e., by 1.974 mm. As previously mentioned in Section III, the vertical resolution of 3 mm is not sufficient to model the Yagi antenna of about 12 mm height accurately. We have, therefore, subdivided the thickness between each of the sections of the new model into two halves, each of thickness 1.5 mm. The complex tissue properties ε_r and σ are thus prescribed for new cells of dimensions $1.974 \times 1.974 \times 1.5$ mm. An unfortunate result of the forward tilt is that the head model now resides in a somewhat larger volume that can be represented by $146 \times 98 \times 176$ cells in x, y, and z directions, respectively.

The Yagi antennas modeled for the SAR calculations are as follows:

1. *Antenna 1*

The geometrical arrangement for this antenna is shown in Fig. 5, where all of the dimensions are marked in terms of the cell sizes $\delta_x = \delta_y = 1.974$ mm, and $\delta_z = 1.5$ mm. For this antenna, the height of the driven element is 12 mm and that for the strip reflector is 24 mm. The width of the strip reflector is 11.8 mm and the spacing between the two elements is 11.8 mm. As shown in Fig. 5, the antenna is mounted on the top of a metallic box of dimensions $5.59 \times 4.83 \times 16.38$ cm in x, y, and z directions, respectively. In our nomenclature, x direction is from front to back, y direction is from side to side, and z direction is from top to bottom of the head. The antenna is centrally located with equal

distance from the two faces in the x direction and mounted such that the strip reflector is at a distance of 11.8 mm from the side of the box that is placed against the ear lobe.

3. *Antenna 2*

This antenna, together with the supporting metallic chassis, is sketched in Fig. 6. All of the dimensions in Fig. 6 are shown in terms of the cell sizes that were used for the model and the antenna. As indicated previously in Section III, the cell sizes δ_x, δ_y, and δ_z used for the various directions are 1.974, 1.974, and 1.5 mm, respectively. As seen in Fig. 6b, the driven elements D and D′ for both the transmitting (T) and receiving (R) antennas are displaced by 2 cells relative to the center line (in xy plane) of the strip reflector.

5. *Antenna 3*

This antenna sketched in Fig. 7 is similar to Antenna 2 except that a somewhat wider and taller reflector is used. The width and height of the strip reflector are taken to be $4\,\delta_x$ (7.9 mm) and $10\,\delta_z$ (15 mm), respectively. Unlike Antenna 2, the driven element of this antenna is assumed to be centrally located relative to the reflector in the xy plane (see Fig. 7b). Also, the reflector is not assumed to be bent back as it is for Antenna 2 (see Fig. 6b).

For each of the calculations, half of the model of the tilted head closest to the handset held either on the right side or on the left side is modeled in a grid of $146 \times 50 \times 176 = 1{,}284{,}800$ cells, each of dimension $1.974 \times 1.974 \times 1.50$ mm along x, y, and z directions, respectively. The axes x, y, and z for the model (and the calculation space) are selected to be from front to back, side to side, and top to bottom of the head, respectively. Together with the model of the handset, the interaction space used for the FDTD calculations is modeled by $158 \times 84 \times 188 = 2{,}495{,}136$ cells. For this model, layer no. 69 is in the same plane as the bottom of the driven antenna.

For the SAR calculations we have normalized the results to 0.6 W input power for the handset. The layer-averaged SARs calculated for Antennas 1, 2, and 3 are shown in Figs. 8a, 8b, and 8c, respectively. While the handset placed against the right ear has been